

Sandwiched three-port grating based on metal-mirror configuration

CHEN FU, BO WANG*, WENHUA ZHU, JIMIN FANG, ZIMING MENG, ZHAOGANG NIE, XIANGJUN XING, LI CHEN, LIANG LEI, JINYUN ZHOU

School of Physics and Optoelectronic Engineering, Guangdong University of Technology, Guangzhou 510006, China

We design and optimize the sandwiched three-port grating based on metal-mirror configuration under normal incidence. By using the rigorous coupled-wave analysis, grating parameters are analyzed and calculated, including grating groove depth, thickness of connecting layer, and so on. Such a new grating is aimed to separate energies into the 0th and the ± 1 st orders for both TE and TM polarizations. Based on the optimized grating parameters, efficiencies can reach more than 32% for each port with the polarization-independent property. It indicates that reflection three-port beam splitter with high efficiency can be obtained by the sandwiched grating.

(Received January 10, 2019; accepted October 9, 2019)

Keywords: Sandwiched grating, Three-port, Metal-mirror configuration, Reflective efficiency

1. Introduction

As an important component in optical system, the beam splitter can divide light into several beams and propagate in different directions [1-6]. It can be used in many practical applications, including photonic integrated circuits [7], calibration of quantum key distribution systems [8], communication devices [9], optical power divider [10], and so on. Grating, as one of the most basic spectroscopic elements, has always attracted widespread attention [11-16]. More importantly, in recent decades, due to the development of micro-fabrication technology, especially photolithography technology, fabricating sub-wavelength grating has become feasible and economical [17]. Diffraction grating is more suitable for miniaturization and integration because of its compact size compared with traditional optical elements. Therefore, diffraction gratings have attracted more and more attention and are widely used in various optical systems, such as coherent beam combination [18], grating couplers [19-22], grating sensor [23-25], light emitting diodes [26], waveguide grating antenna [27], communication [28,29], and so on.

In the past decades, the grating diffraction theory has formed a relatively perfect theoretical system. The rigorous coupled-wave analysis (RCWA) is an appropriate method to optimize the grating profile, which can calculate exact grating parameters [30]. In addition, the development of lithography technology has been applied to the fabrication of subwavelength gratings, which makes more and more researchers pay attention to the research of subwavelength gratings. Feng *et al.* designed and fabricated the deep-etched polarization-independent binary fused-silica phase grating as a three-port beam splitter [31]. Although the diffraction efficiency of the grating is

relatively high, the beam splitting effect of the grating is not good enough. Later, Li *et al.* were inspired to design the three-port beam splitter of sandwiched fused-silica grating based on RCWA method [32]. By adding a covering layer, the beam splitting effect is better.

In this paper, the sandwiched grating based on metal-mirror configuration is proposed for three-port beam splitter. Complex grating structure includes grating region to achieve diffraction, covering layer to reduce Fresnel loss, connecting layer to achieve broadband characteristics, and metal plate to achieve reflection of incident wave. The sandwiched grating has good beam splitting ratio uniformity for both TE and TM polarizations. It can divide the incident wave the ± 1 st and the 0th reflection orders for the polarization-independent beam splitter. The RCWA is used to optimize the grating parameters including the grating depth and the thickness of the connecting layer, efficiencies more than 32% for each diffractive order can be realized. Therefore, for practical applications, the sandwiched grating would be a useful device for future practical applications.

2. Numerical design

The graphical representation of the sandwiched three-port grating based on metal-mirror configuration is shown in Fig. 1. The sandwiched grating consists of silica cover, grating layers, connecting layer, the silver reflector and fused-silica substrate. The grating parameters include the grating period of d , grating ridge breadth of a , the grating groove depth of h_g , the connecting layer thickness of h_c , and the silver interlayer thickness of h_m . The Ag slab with its refractive index of $n_m = 0.469 - 9.32i$ is located below the connection layer. The interior of the grating grooves is air with refractive index of $n = 1.0$. Except for

the Ag slab and the grating grooves, the other grating materials are fused silica with refractive index of $n_1 = 1.45$. Duty cycle f is the ratio of a to d . Under the condition of vertical incidence, the plane wave with wavelength of $\lambda=1550$ nm is incident on the novel grating.

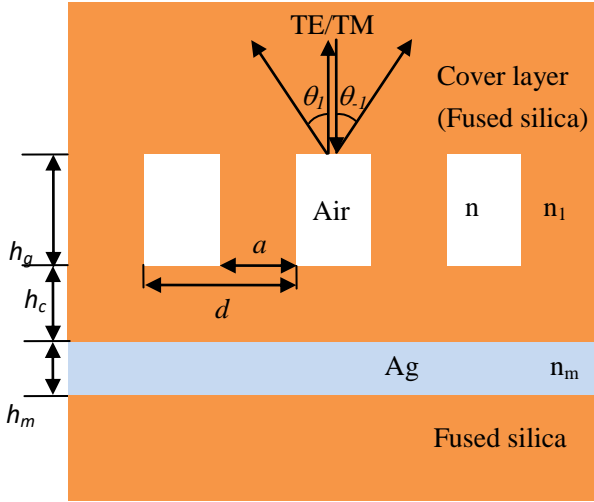


Fig. 1. (Color online) Schematic of the sandwiched three-port grating based on metal-mirror configuration

Through the grating of the incident wave can be transmitted to different direction, the propagation direction can be determined by grating equation:

$$n_{out} \sin(\theta_i) = n_{in} \sin(\theta) + i\lambda/d \quad (1)$$

In this equation, n_{out} is the refractive index of the export medium and n_{in} is the refractive index of the incident medium. θ_i depicts an angle of the i th diffractive order, and θ is the incident angle. In order to make the grating a three-port beam splitter under vertical incidence, only three diffraction orders of the 0th, the 1st, and the -1st should be ensured. Because of the symmetry of incident light and rectangular gratings, the energy of the 1st order and the -1st order are the same in these three orders. Therefore, only the diffraction efficiency of the -1st order and the 0th order need to be considered.

In order to facilitate production, we set the duty cycle to 0.5. It has been found that when the thickness of the silver plate exceeds $0.1 \mu\text{m}$, the metal plate can completely reflect the incident light. In addition, through a large number of simulation calculations, we choose the grating period d of 1920 nm.

According to RCWA method, the thickness of connecting layer h_c and grating groove depth h_g are optimized by numerical calculation method to achieve higher reflection efficiency. Fig. 2 shows efficiency versus grating depth layer and thickness of connecting layer with the grating duty cycle of 0.5 and grating period of 1920 nm for working wavelength of 1550 nm under vertical incidence. The four figures show diffraction efficiencies of TE and TM polarizations in the 0th order and the -1st orders. When grating groove depth h_g is $1.57 \mu\text{m}$ and

connecting layer thickness h_c is $1.63 \mu\text{m}$ and grating period of 1920 nm, the TE polarized light can be separated with efficiencies of 32.30% and 32.38% in the 0th order and the -1st order, respectively. For TM-polarized light, efficiencies of 32.3% and 32.26% can be separated into the 0th order and the -1st order, respectively.

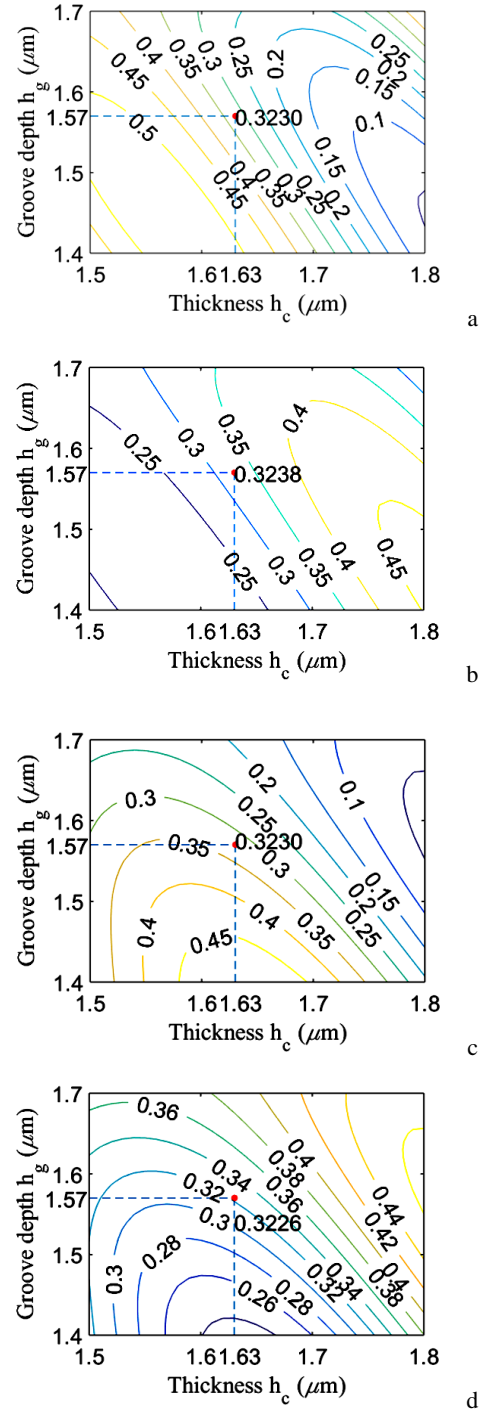


Fig. 2. (Color online) Diffraction efficiency versus grating depth and thickness of the connecting layer with the grating duty cycle of 0.5 and grating period of 1920 nm at working wavelength of 1550 nm under normal incidence: (a) TE polarization in the 0th order, (b) TE polarization in the -1st order, (c) TM polarization in the 0th order, (d) TM polarization in the -1st order

3. Results and discussion

By using RCWA method, the optimum parameters of the grating are obtained, the efficiency of TE polarized light reaches 97.08%, while that of TM polarized light reaches 96.82%. But in actual production, in order to facilitate manufacturing, we also need to consider the redundancy of grating parameters.

Fig. 3 displays the diffraction efficiency versus the duty cycle with grating period of 1920 nm under normal incidence. As shown in Fig. 3, the diffraction efficiency of the grating will also change due to the change of the duty cycle of the grating. When the duty cycle is 0.5, the grating can make TE polarized light and TM polarized light achieve the excellent beam splitting effect. In the actual manufacturing of grating etching, the manufacturing tolerance is taken into account, when the duty cycle is in the range of 0.489 to 0.509, for both TE and TM polarizations in each diffractive order, the diffraction efficiencies of the grating are higher than 30%.

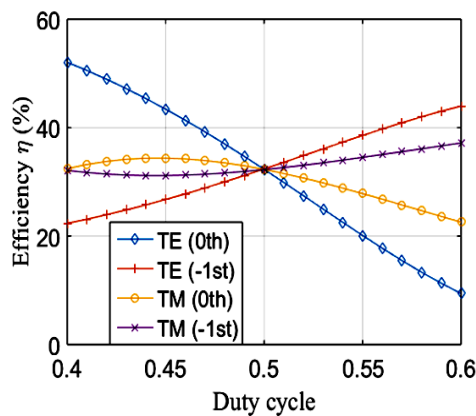


Fig. 3. (Color online) Efficiency versus grating duty cycle for the sandwiched grating with the optimized parameters at the working wavelength of 1550 nm under normal incidence

In the practical fabrication of gratings, besides the tolerance of duty cycle, the redundancy of grating period should also be considered. Fig. 4 displays the transmission efficiency versus the grating period under normal incidence. When the grating period is in the range of 1910 nm to 1932 nm, for both TE and TM polarizations in each diffractive order, the diffraction efficiencies of the grating are higher than 30%. The grating of the grating period has a relatively wide tolerance, which is beneficial to the actual industrial production.

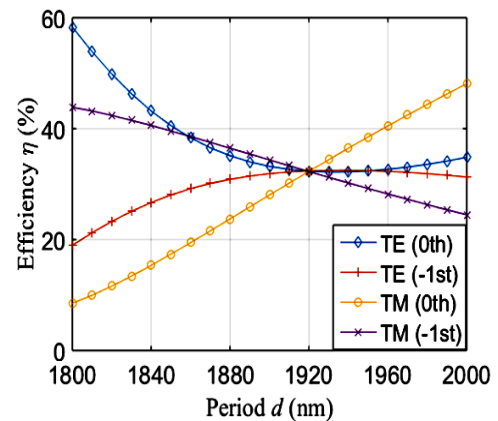


Fig. 4. (Color online) Diffraction efficiency versus grating period with the grating duty cycle of 0.5 at the working wavelength of 1550 nm under normal incidence

Similarly, using RCWA method, we can study wide wavelength bandwidth and angle range. The diffraction efficiency of sandwiched gratings varies with the incident wavelength and angle. Fig. 5 shows the efficiency with different incident wavelengths for the optimized grating parameters using RCWA. In Fig. 5, with deviation of the central incident wavelength, a broad incident wavelength bandwidth can be obtained for TE-polarized wave within range of 1545–1560 nm, where efficiencies in the ± 1 st orders and the 0th order can be more than 30%.

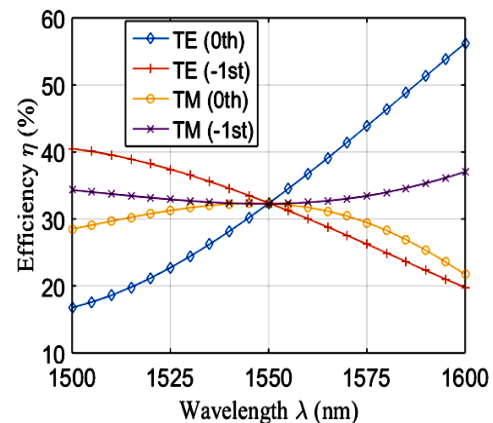


Fig. 5. (Color online) Diffraction efficiency versus incident wavelength for the sandwiched beam splitter by metal-mirror-based binary grating under normal incidence

Fig. 6 shows the incident wave illuminates the reflective three-port beam splitter grating at an incidence angle near normal incidence for a wavelength of 1550 nm. When the incident light is normal incidence, the grating can make TE polarized light and TM polarized light achieve the best beam splitting effect. In Fig. 6, when the incident angle is in the range -0.1 – 0.1° , the beam splitting performance of the grating is good, and the diffraction efficiency is more than 30%.

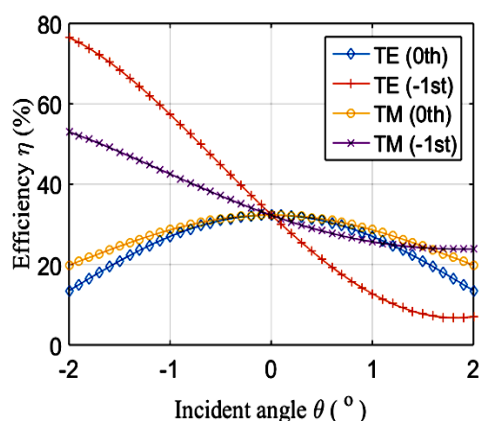


Fig. 6. (Color online) Diffraction efficiency versus incident angle with the optimized grating profile

4. Conclusion

In conclusion, the polarization independent three-port beam splitter grating designed and optimized has the advantages of high efficiency, good beam splitting and wide incident bandwidth. The grating groove depth and thickness of the connecting layer are numerically optimized accurately using the RCWA. With the grating groove depth of $1.57 \mu\text{m}$ and connecting layer thickness of $1.63 \mu\text{m}$ for the incident wavelength of 1550 nm under normal incidence, the TE polarized light can be separated the efficiencies of 32.30% and 32.38% in the 0th order and the -1st order, respectively. For TM-polarized light, efficiencies of 32.3% and 32.26% can be separated into the 0th order and the -1st order, respectively. When operation for different incident wavelength and angle, the bandwidth for operation can be exhibited to some extent. For incident wavelength, the bandwidth is 22 nm . As an efficient three-port splitter, the grating can meet the requirements of different optoelectronic devices and will be a promising device.

Acknowledgements

This work is supported by the National Natural Science Foundation of China (61675050, 11774071, 11774069).

References

[1] M. Singh, *Optik* **178**, 902 (2019).
 [2] Q. Zhang, M. Li, T. Liao, X. Cui, *Opt. Commun.* **411**, 93 (2018).
 [3] W. Zhu, B. Wang, H. Li, K. Wen, Z. Meng, Q. Wang, X. Xing, L. Chen, L. Lei, J. Zhou, *Optoelectron. Adv. Mat.* **12**(11-12), 629 (2018).

[4] H.-C. Yuan, X.-X. Xu, Y.-J. Xu, *Optik* **172**, 1034 (2018).
 [5] S. Lv, J. Jing, *Opt. Commun.* **424**, 63 (2018).
 [6] A. Fedouche, H. A. Badaoui, M. Abri, *Optik* **157**, 1300 (2018).
 [7] H. Saghaei, A. Zahedi, R. Karimzadeh, F. Parandin, *Superlattices Microstruct.* **110**, 133 (2017).
 [8] Y.-Y. Fei, X.-D. Meng, M. Gao, Z. Ma, H. Wang, *Optik* **170**, 368 (2018).
 [9] J. Ren, X. Sun, S. Wang, *Superlattices Microstruct.* **116**, 221 (2018).
 [10] G. Fan, Y. Li, B. Han, *IEEE Photon. J.* **9**(6), 6601905 (2017).
 [11] M. Gambhir, S. Gupta, *Optik* **164**, 567 (2018).
 [12] R. Wang, T. Sang, L. Wang, J. Gao, Y. Wang, J. Wang, *Optik* **157**, 651 (2018).
 [13] G. Zhou, W. Tian, *Optik* **172**, 1104 (2018).
 [14] Y. Dai, H. Xu, H. Wang, Y. Lu, P. Wang, *Opt. Commun.* **416**, 66 (2018).
 [15] B. Zhang, Y. Liu, Z. Zhao, P. Yan, *Opt. Commun.* **427**, 48 (2018).
 [16] J. Lu, B. Ding, Y. Huo, T. Ning, *Opt. Commun.* **415**, 146 (2018).
 [17] H. Hao, Z. Tingting, S. Qing, Y. Xiaodong, *Opt. Commun.* **434**, 28 (2019).
 [18] S. Li, Y. Lu, *Opt. Commun.* **407**, 321 (2018).
 [19] C. Wan, T. K. Gaylord, M. S. Bakir, *IEEE Photon. Technol. Lett.* **29**(21), 1776 (2017).
 [20] T. Sharma, H. Kwon, J. Park, S. Han, G. Son, Y. Jung, K. Yu, *Opt. Commun.* **427**, 452 (2018).
 [21] J. H. Song, X. Rottenberg, *IEEE Photon. Technol. Lett.* **29**(4), 389 (2017).
 [22] L. Liu, Q. Deng, Z. Zhou, *IEEE Photon. Technol. Lett.* **29**(22), 1927 (2017).
 [23] H. Deng, P. Lu, S. J. Mihailov, J. Yao, *J. Lightwave Technol.* **36**(23), 5587 (2018).
 [24] D. Guo, H. Jiang, L. Shi, M. Wang, *IEEE Photon. J.* **10**(1), 6800609 (2018).
 [25] K. Yang, Y. Liu, Z. Wang, Y. Li, Y. Han, H. Zhang, *IEEE Photon. J.* **10**(3), 7102708 (2018).
 [26] T. Iqbal, *Curr. Appl. Phys.* **18**(11), 1381 (2018).
 [27] K. Han, V. Yurlov, N. E. Yu, *Curr. Appl. Phys.* **18**(7), 824 (2018).
 [28] W. Feng, Z. Gu, *IEEE Photon. Technol. Lett.* **30**(15), 1361 (2018).
 [29] M. Ma, Z. Chen, H. Yun, Y. Wang, X. Wang, N. A. Jaeger, L. Chrostowski, *IEEE Photon. Technol. Lett.* **30**(1), 111 (2018).
 [30] M. G. Moharam, D. A. Pommet, E. B. Grann, T. K. Gaylord, *J. Opt. Soc. Am. A* **12**(5), 1077 (1995).
 [31] J. Feng, C. Zhou, B. Wang, J. Zheng, W. Jia, H. Cao, P. Lv, *Appl. Opt.* **47**(35), 6638 (2008).
 [32] H. Li, B. Wang, H. Pei, W. Shu, L. Chen, L. Lei, J. Zhou, *Int. J. Mod. Phys. B* **30**(12), 1650072 (2016).